Preparation of Highly Monodisperse Droplet in a T-Junction Microfluidic Device

J. H. Xu, S. W. Li, J. Tan, Y. J. Wang, and G. S. Luo
The State Key Lab of Chemical Engineering, Dept. of Chemical Engineering, Tsinghua University, Beijing 100084, China

DOI 10.1002/aic.10924
Published online June 15, 2006 in Wiley InterScience (www.interscience.wiley.com).

In our previous work, a new flow route was developed—a so-called perpendicular shear force–induced droplet formation—in a self-designed simple T-junction microchannel device. In this work, the crossflowing rupture technique was used to prepare monodisperse droplets in a similar device and successfully prepared monodisperse droplets ranging from 50 to 500 μm with polydispersity index (σ) values of <2%. Two kinds of flow patterns of plug flow and drop flow in the T-junction microchannels could be formed. By changes in the surfactant concentration, the interfacial tension and the wetting ability varied, and the disordered or ordered two-phase flow patterns could be controlled. Evolutions of the contact angle of the oil in contact with the wall surface were explained by the adsorption of surfactant molecules to the solid–liquid interface. The increase of continuous phase flow rate and viscosity resulted in the decrease of the droplet size, and the droplet size was correlated with capillary number Ca. By comparing the variation range of drop size using the two methods, it was found that the method of perpendicular flow-induced droplet formation can control the drop size over a much wider range. © 2006 American Institute of Chemical Engineers *AIChE J,* 52: 3005–3010, 2006
Keywords: monodisperse droplet, crossflowing rupture technique, microfluidic device

Introduction

Emulsions are important materials and products in food, pharmaceutical, cosmetics, and chemical industries. The droplet size and distribution are the most important parameters that affect the stability, rheology, chemical reactivity, and physiological efficiency of any emulsion. Monodisperse emulsions have received a great deal of attention because of their improved stability and facilitated control of their properties. Conventional emulsification techniques use inhomogeneous extensional and shear flows to rupture droplets, commonly resulting in droplets with a wide size distribution. Several strategies have been proposed to reduce the polydispersity of droplets.[1,2] Recently, the remarkable development of micromachining technology over the last decade led to the fabrication of miniature embedded systems involving many micromachined components and structures. Moreover, the growing trends in the miniaturization of experimental systems have facilitated the expansion of droplet-based applications from the traditional emulsions to microanalysis, on-chip separation, and chemical and biochemical microreactions.[3-6] In these devices, the control of small volumes of fluids and the understanding of multiphase flows are required. Monodisperse droplets in microfluidic devices have been generated by a number of methods, including geometry-dominated breakup,[7-9] crossflowing rupturing through a micropore or microchannel array,[10,11] perpendicular flow–induced breakup,[12] hydrodynamic flow focusing through a small orifice,[13-15] and crossflowing rupture in a T-junction microchannel.[16-20] Further, highly uniform emulsion droplets with standard deviations < 5% can alternatively be generated.[14,16,20] Despite the significant advances made in the past few years, major challenges remain in the development of microchannel droplet formation techniques and mechanisms, such as the quantitative effects of flow rates, viscosities and the interfacial tension on droplet formation process, and effects of wetting properties on two-phase flow patterns.

Correspondence concerning this article should be addressed to G. S. Luo at gsluo@tsinghua.edu.cn.

In our previous work, we developed a new flow route: a so-called perpendicular shear force–induced droplet formation in T-junction microchannels.[12] A quartzose capillary was embedded into the perpendicular channel. The continuous (water) phase flow was introduced from the perpendicular quartzose capillary channel and the dispersed (oil) flow from the horizontal channel, so the droplet formation method was designated a *perpendicular shear force* technique. We also ascertained that the wetting properties of the fluid with the walls are exceedingly important parameters. In this article, we used a similar T-junction microchannel device to prepare monodisperse droplets using the crossflowing rupture technique. The continuous (water) phase flow was introduced from the horizontal channel and the dispersed (oil) flow from the perpendicular quartzose capillary channel, so the droplet formation method was designated a *crossflowing rupture* technique. We investigated the effects of the surfactant concentration, flow rates, and continuous-phase viscosity on the droplet formation process. We qualitatively explained the effect of surfactant concentration on the wetting property between the dispersed phase and the wall surface. The difference of effects of experimental conditions on droplet size by using perpendicular shear force induced droplet formation and crossflowing rupture techniques is investigated and compared. Additionally, the droplet formation mechanism is discussed.

Experimental

Microfluidic device

The experiments were performed in a T-junction microchannel device fabricated on a polymethyl methacrylate (PMMA) sample plate (100 × 20 × 5 mm) using an end mill. The continuous (water) phase flow channel dimensions were about 300 × 200 μm (width × height). A quartzose capillary (inner diameter = 50 μm) was embedded into the perpendicular channel [200 × 200 μm (width × height)] as the dispersed (oil) flow channel. The measured channel dimensions were about 400 × 400 μm (width × height) (Figure 1). After that, the microfluidic device was sealed using another PMMA thin plate (1 mm in thickness). Finally, the microfluidic chip was sealed by curing at 105°C using high-pressure thermal sealing techniques. Two microsyringe pumps and two gastight microsyringes were used to pump the two phases into the microfluidic device, respectively.

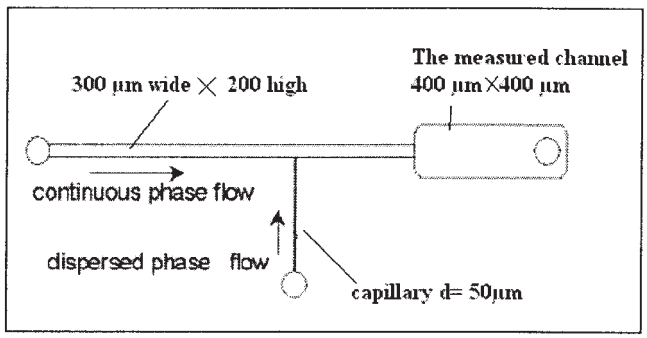

Figure 1. The crossflowing microfluidic device.

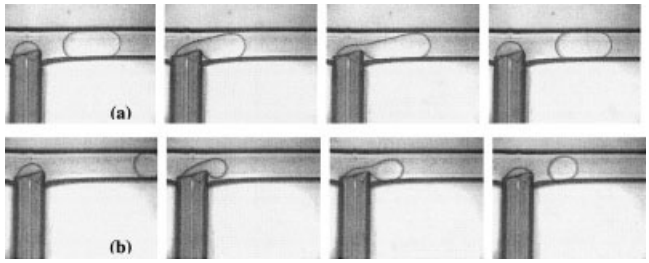

Figure 2. Micrographs of the oil–water interface at the intersection channel during droplet formation processes.

(a) Oil-phase flow rate = 3 μL/min; water-phase flow rate = 15 μL/min. (b) Oil-phase flow rate = 3 μL/min; water-phase flow rate = 80 μL/min.

Materials

n-Octane was used as the dispersed phase; deionized water was used as the continuous phase. Different concentrations of sodium dodecyl sulfate (SDS) used as the surfactants were added into the water phase. SDS concentrations ranged from 0.001 to 1.0 wt % to control the interfacial tension between the water and oil phases. The surfactant molecules tend to collect at the two-phase interface, with their polar heads in the water phase and their tails in the oil phase. Glycerol was used to control the viscosities of the water phase. In our experiments, three different glycerol concentrations of 24, 52, and 62 wt % were used.

Visualization and analysis

Experiments were carried out with a microscope at magnifications from 20× to 200×. A high-speed CCD video camera was connected to the microscope and the images were recorded at a frequency of 200 images/s. The length of oil plugs or the diameter of oil drops at the channel was measured from microscope images. After changing any of the flow parameters, we allowed at least 100 s of equilibration time. The average droplet size (d_{av}) and the polydispersity index (σ) were determined by measuring the sizes of at least 100 drops from recorded pictures using custom-made image-analysis software. σ is defined by the following equation:

$$\sigma = \delta/d_{av} \times 100\% \quad (1)$$

where σ is the polydispersity index, δ is the standard deviation, and d_{av} is the average droplet diameter.

Results and Discussion

Monodisperse droplet formation and its distribution

Monodispersed droplet formation was tested by pumping the oil and the water phases into the capillary and continuous-phase flow channel, respectively. Figure 2 gives four pictures of the droplet formation process in the microchannel device for two different experimental conditions, respectively. At a low water-phase flow rate of 15 μL/min, the continuous shear force was low and only induced the oil phase to isolate plugs because their diameters were greater than the microchannel width. When we increased the water-phase flow rate (Q_w) to 80

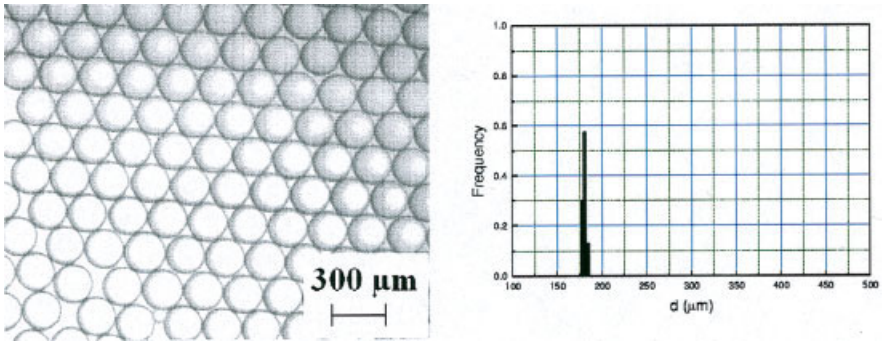

Figure 3. Micrographs of monodisperse drops and droplet size distribution.

The continuous phase was 0.5% SDS and 52% glycerol–water aqueous solution. Interfacial tension = 2.54 mN m^{-1}; continuous phase viscosity = 6.1 mPa·s. Oil-phase flow rate = 5 μL/min; water-phase flow rate = 80 μL/min. Average droplet size d_{av} = 181.4 μm; the polydispersity index (σ) = 1.5%. [Color figure can be viewed in the online issue, which is available at www.interscience.wiley.com]

μL/min, drops as spheres could be observed. Thus we could easily obtain regular oil–water plug flow and drop flow patterns by varying the two-phase flow rates. Figure 3 shows micrographs of monodisperse drops and droplet size distributions. The formed drops had a spherical shape with regular size. We varied the experimental conditions, such as water-phase flow rate, oil-phase flow rate, and continuous-phase viscosity; the droplet size was highly uniform and the polydispersity index (σ) values were <2% for all of our experimental results.

Previous studies for liquid–liquid systems show that the droplet size is affected by viscosity, interfacial tension, two-phase flow rates, and wetting properties.[10-12,16-18] Therefore, we quantitatively investigated in detail the effects of surfactant concentration, two-phase flow rates, and continuous-phase viscosity.

Effect of surfactant concentration

In our previous work, we found that the wetting properties of the liquids, with respect to the wall surfaces, deserve particular emphasis.[12] In this work, we also examined how the surfactant concentrations affect two-phase flow properties in the cross-flowing rupture process by using the water phase with different concentrations of SDS in our experiments. Figure 4 shows the effect of surfactant concentration on the two-phase flow properties when the oil flow rate was 10 μL/min and the water flow rate was 20 μL/min. At lower surfactant concentrations (<0.04% w/w), disordered states were reached and the oil phase partially adhered to the channel walls. At higher concentrations (>0.05% w/w), well-defined oil plugs were formed, continuously moving with the water-phase flow. It can thus be concluded that the wetting properties between oil and wall surface determine whether the ordered flow of oil drops can be obtained. This result is similar to the perpendicular flow–induced monodisperse droplet formation process.[12] The evolutions of the contact angle of the oil in contact with the wall surface may be explained by the adsorption of surfactant molecules to the solid–liquid interface, shown in Figure 5. To form an oil-in-water system with oil phase as the dispersed phase, the channel wall must show hydrophilic performance, although PMMA is characteristically hydrophobic. By adding surfactant into the water phase, the surfactant molecules begin to be adsorbed with their polar heads in the water phase and their tails on the wall surface, thus changing the wall wetting ability. When the SDS concentration is greater than the critical micelle concentration (CMC) value, the wall surface will be totally hydrophilic. This shift is critically important: to form ordered patterns, one must start with surfactant concentrations well above the CMC. Thus in our subsequent experiments, the surfactant concentration was maintained at 0.5% w/w.

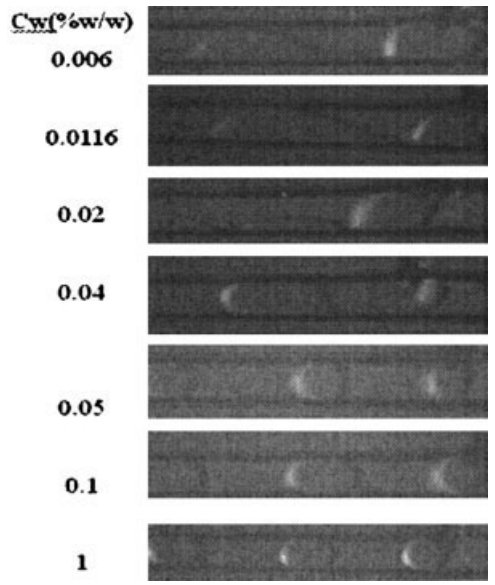

Figure 4. Effect of surfactant concentration on two-phase flow patterns.

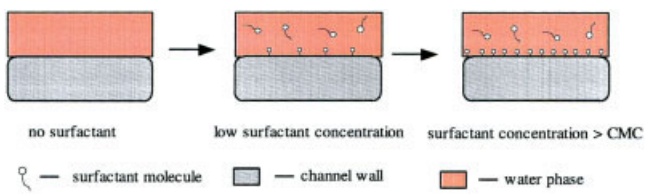

Figure 5. Mechanism scheme that illustrates the effect of adsorption of surfactant molecules on the wetting property.

[Color figure can be viewed in the online issue, which is available at www.interscience.wiley.com]

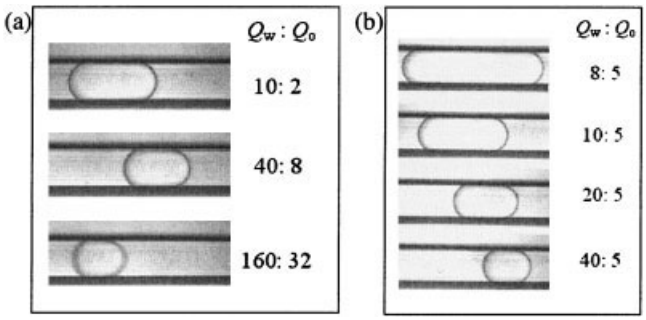

Figure 6. Micrographs illustrating the influences of two-phase flow rates on oil plugs.

(a) Total flow rate and (b) water flow rate. The units of flow rates in the figures are all in microliters per minute (μL/min).

Effects of two-phase flow rates and continuous-phase viscosity on droplet size

Figures 6a and 6b show the micrographs of oil plugs under different total flow rates at a fixed value of Q_w/Q_o and under different water-phase flow rates with a fixed oil flow rate of 5 μL/min, respectively. Figures 7a and 7b show the effects of total flow rate and values of Q_w/Q_o on oil plug length. The plug length decreases with increasing Q_w/Q_o ratio (Figures 6b and 7b) and total flow rate (Figures 6a and 7a). In a previous perpendicular shear droplet breakup process, using a similar device, the plug length is affected only by the value of Q_w/Q_o, but is independent of the total flow rate.[12] Table 1 shows a comparison of relative plug size by using perpendicular flow–induced droplet formation and crossflowing rupture techniques. It can be seen that the values of relative length are smaller by using crossflowing rupture technique under the same experimental conditions. The most likely reason for the difference is that the continuous-phase flow shear force is predominant in the crossflowing rupture process, whereas the wall effects and interfacial tension are more predominant in the perpendicular shear droplet breakup process when the droplet diameter is larger than the microchannel width.

Furthermore, we investigated the effects of two-phase flow rates on droplet diameter as two-phase flow pattern was in the drop flow regime. Figures 8a and 8b show the micrographs of oil drops in different total flow rates at a fixed value of Q_w/Q_o and in different water-phase flow rates at a fixed oil flow rate of 5 μL/min, respectively. Figure 9 shows the effects of two-phase flow rates on oil average droplet diameter d_{av}. The drop diameter decreases with increasing Q_w, whereas the oil-phase flow rate Q_o has only a slight influence on droplet size. Drop diameter also decreases with increasing total flow rate. Table 2 provides a comparison of droplet sizes by using perpendicular flow–induced droplet formation and crossflowing rupture techniques. The average droplet diameters are larger by using crossflowing rupture technique under the same experimental conditions. The main reason is that the continuous-phase flow shear force is much higher in the perpendicular flow–induced droplet formation process under the same continuous flow rates.

Table 1. Comparison of Plug Lengths under the Same Conditions by Using Perpendicular Flow Rupture and Crossflowing Rupture Techniques

			Relative Length (l/w)	
No.	Continuous Phase	Q_o:Q_w (μL min^{-1})	Perpendicular Flow Rupture[12]	Crossflowing Rupture
(1)	0.5% SDS/Water	10:10	4.10	2.94
(2)	0.5% SDS/Water	10:20	2.80	2.28
(3)	0.5% SDS/Water	10:60	1.79	1.17

Figure 10 shows the effect of the continuous-phase viscosity on the average droplet size when the continuous phases contain different concentrations of glycerol with 0.5 wt % SDS. The continuous-phase viscosities range from 0.92 to 10.84 mPa·s. The average droplet size also decreases with increasing continuous-phase viscosity. These results are similar to previous droplet formation processes in T-junction microchannels.[10-12,16,17]

Discussion of droplet formation mechanism

In previous reports of the crossflowing rupture droplet formation process, the physical model to predict the droplet size is based primarily on the balance of shear force caused by continuous-phase flow and Laplace pressure caused by interfacial tension.[16,20] A dimensionless number—the capillary number (Ca), which is the ratio of viscous-to-interfacial tension stress—can be used to predict the droplet diameter:

$$Ca = \mu_c u_c / \gamma \tag{2}$$

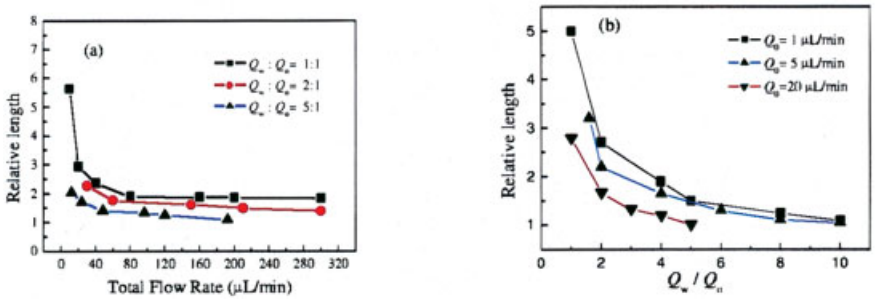

Figure 7. Influences of two-phase flow rates on length of oil plugs.

(a) Total flow rate and (b) ratio of water and oil flow rate. All measurements of length are reported relative to the width of channels (300 μm). Relative size is defined as the ratio of plug length to channel width. [Color figure can be viewed in the online issue, which is available at www.interscience.wiley.com]

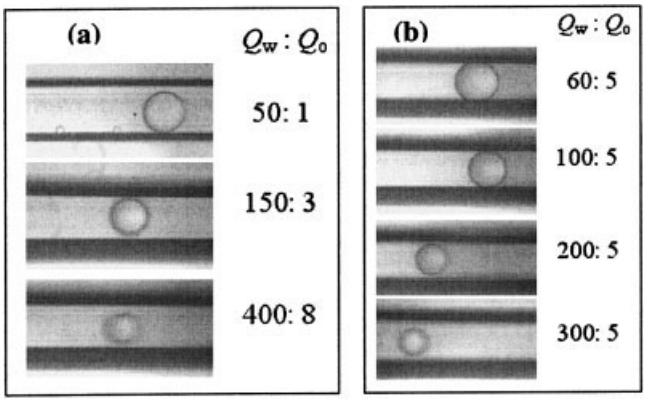

Figure 8. Micrographs illustrating the influences of two-phase flow rates on size of oil drops.

(a) Effect of total flow rate when the value of Q_w/Q_o retained is 50:1. (b) Effect of water flow rate at a fixed oil flow rate of 5 μL/min. The units of flow rates in the figures are all μL/min.

where μ_c is the viscosity of continuous flow (here the water phase), γ is the oil/water interfacial tension, and u_c is the velocity of continuous flow in the microchannel (here the water phase). The drops diameter is then described by

$$d_{av} \propto 1/Ca \tag{3}$$

From Eqs. 2 and 3 the droplet diameter decreases with increasing Q_w and continuous-phase viscosity μ_c, which is in agreement with our experimental results. Figure 11 shows the relationship between average droplet size and the value of capillary number Ca under different experimental conditions. Figure 11 reveals that droplet sizes fall within theoretical scaling (Eq. 3) when $d_{av} < h$, where h is the height of microchannel, whereas the droplet sizes scale with Ca as $d_{av} \propto Ca^{-0.3}$ when $d_{av} > h$. That is, when the droplet size is less than the microchannel height, droplets are sufficiently small that the hydrodynamic forces exerted by the channel walls are not important and breakup fully relies on the straining of the imposed flow. When the droplet diameter is larger than the channel height, wall effects are dominant over the stresses directly imposed by the flow, and the dependency of droplet sizes on flow rate is weaker. Thus the theoretical study on the

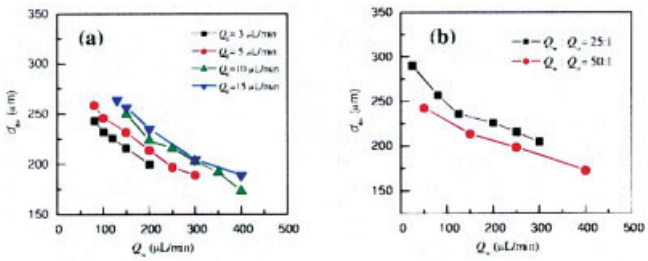

Figure 9. Influences of two-phase flow rates on the average oil droplet diameter.

The continuous phase was 0.5 wt % SDS aqueous solution in these experiments and the interfacial tension $\gamma = 2.54$ mN/m, continuous phase viscosity $\mu = 0.92$ mPa·s. [Color figure can be viewed in the online issue, which is available at www.interscience.wiley.com]

Table 2. Comparison of Average Droplets Diameters under the Same Conditions by Using Perpendicular Flow Rupture and Crossflowing Rupture Techniques

No.	Continuous Phase	Q_o:Q_w (μL min^{-1})	Average Droplet Size d_{av} (μm)	
			Perpendicular Flow Rupture[12]	Crossflowing Rupture
(1)	0.5% SDS/Water	3:80	130	245
(2)	0.5% SDS/Water	3:100	100	230
(3)	0.5% SDS/Water	3:150	60	210

effect of channel wall when the drop size is larger than the channel size should be an urgent work.

Conclusions

We developed a T-junction microfluidic device with a capillary as the dispersed flow channel to produce monodisperse emulsions, and successfully prepared monodisperse droplets ranging from 50 to 500 μm with polydispersity index (σ) values of <2%. We investigated the parameters affecting the droplet formation process, such as surfactants, two-phase flow rates, and continuous phase viscosity, and the droplet formation mechanism was discussed. In our experiments, wetting properties of the fluid to the walls could determine the two-phase flow conditions. Only when the contact angle is >90°, can the flow of ordered drops be formed. Evolutions of the contact angle of the oil in contact with the wall surface were explained by the adsorption of surfactant molecules to the solid–liquid interface. The drop diameter decreases with increasing Q_w, total flow rate, and continuous-phase viscosity, which is similar to results of a previous study. By fitting the relationship between droplet size d_{av} and capillary number Ca, we found the different scaling law of droplets in two different regions. When d_{av} is less than the height of microchannel h, droplet sizes fall in the theoretical scaling of $d_{av} \propto 1/Ca$; when $d_{av} > h$, the droplet sizes scale with Ca as $d_{av} \propto Ca^{-0.3}$. The primary reason

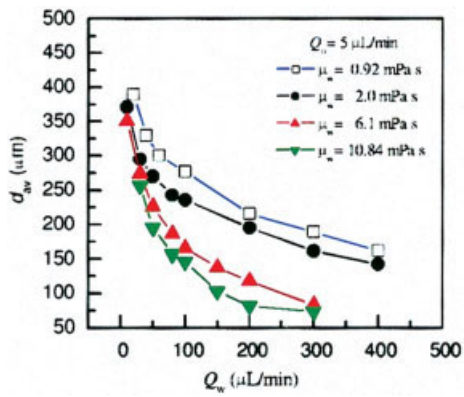

Figure 10. Effects of continuous-phase viscosity on the average droplet size in different continuous-phase flow rates when the continuous phases constituted different concentrations of glycerol.

Glycerol concentrations of 24, 52, and 62 wt % were used, respectively. [Color figure can be viewed in the online issue, which is available at www.interscience.wiley.com]

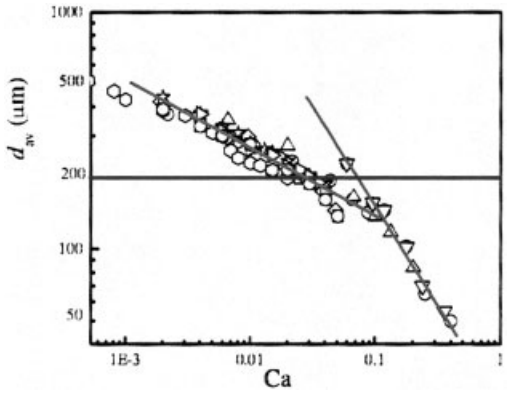

Figure 11. Relationship between average droplet size and the value of capillary number *Ca*.

Symbols correspond to different oil-phase flow rates, water/oil flow ratio, and water-phase viscosities. (□): μ_c = 0.92 mPa·s and Q_o = 3 μL/min; (○): μ_c = 0.92 mPa·s and Q_o = 5 μL/min; (△): μ_c = 6.0 mPa·s and Q_o = 10 μL/min; (▽): μ_c = 10.84 mPa·s and Q_o = 5 μL/min; (◇): μ_c = 2.0 mPa·s and Q_o = 5 μL/min; (☆): μ_c = 0.92 mPa·s and Q_w/Q_o = 5:1; (⬡): μ_c = 0.92 mPa·s and Q_w/Q_o = 2:1. [Color figure can be viewed in the online issue, which is available at www.interscience.wiley.com]

for these phenomena is that wall effects are dominant over the stresses directly imposed by the flow when the droplet diameter is larger than the channel size. The study on scaling law, considering the effect of channel wall when the drops are larger than the channel size, should be an urgent work in future. Compared with the perpendicular shear force–induced droplet formation technique, the variation range of drop size with the crossflowing rupture technique is somewhat narrower.

Acknowledgments

With gratitude we acknowledge the Department of Biological Sciences and Biotechnology in Tsinghua University for providing the microfluidic device. We also gratefully acknowledge the financial support of this work from the National Natural Science Foundation of China, under Grants 20476050, 20490200, 20525622, and the Specialized Research Fund for the Doctoral Program of Higher Education (SRFDP Grant No. 20040003032).

Literature Cited

1. Mason TG, Bibette J. Shear rupturing of droplets in complex fluids. *Langmuir.* 1997;13:4600-4613.
2. Umbanhowar PB, Prasad V, Weitz DA. Monodisperse emulsion generation via drop break off in a coflowing stream. *Langmuir.* 2000;16:347-351.
3. Song H, Ismagilov RF. Millisecond kinetics on a microfluidic chip using nanoliters of reagents. *J Am Chem Soc.* 2003;125:14613-14619.
4. Chen X, Wu H, Mao C, Whitesides GM. A prototype two-dimensional capillary electrophoresis system fabricated in poly(dimethylsiloxane). *Anal Chem.* 2002;74:1772-1778.
5. Burns JR, Ramshaw C. The intensification of rapid reactions in multiphase systems using slug flow in capillaries. *Lab Chip.* 2001;1:10-15.
6. Zheng B, Roach LS, Ismagilov RF. Screening of protein crystallization conditions on a microfluidic chip using nanoliter-size droplets. *J Am Chem Soc.* 2003;125:11170-11171.
7. Kobayashi I, Nakajima M, Chun K, Kikuchi Y, Fujita H. Silicon array of elongated through-holes for monodisperse emulsion droplets. *AIChE J.* 2001;48:1639-1644.
8. Link DR, Anna SL, Weitz DA, Stone HA. Geometrically mediated breakup of drops in microfluidic devices. *Phys Rev Lett.* 2004;92:054503/1-4.
9. Tan YC, Fisher JS, Lee AI, Cristini V, Lee AP. Design of microfluidic channel geometries for the control of droplet volume, chemical concentration, and sorting. *Lab Chip*. 2004;4:292-298.
10. Kawakatsu T, Kikuchi Y, Nakajima M. Regular-sized cell creation in microchannel emulsification by visual microprocessing method. *J Am Oil Chem Soc.* 1997;74:317-321.
11. Xu JH, Luo GS, Chen GG, Wang JD. Experimental and theoretical approaches on droplet formation from a micrometer screen hole. *J Membr Sci.* 2005;266:121-131.
12. Xu JH, Luo GS, Li SW, Chen GG. Shear force induced monodisperse droplet formation in a microfluidic device by controlling wetting properties. *Lab Chip.* 2006;1:131-136.
13. Anna SL, Bontoux N, Stone HA. Formation of dispersions using "flow focusing " in microchannels. *Appl Phys Lett.* 2003;82:364-366.
14. Xu Q, Nakajima M. The generation of highly monodisperse droplets through the breakup of hydrodynamically focused microthread in a microfluidic device. *Appl Phys Lett.* 2004;85:3726-3728.
15. Ward T, Faivre M, Abkarian M, Stone HA. Microfluidic flow focusing: Drop size and scaling in pressure versus flow-rate-driven pumping. *Electrophoresis.* 2005;26:3716-3724.
16. Thorsen T, Roberts R, Arnold F, Quake S. Dynamic pattern formation in a vesicle-generating microfluidic device. *Phys Rev Lett.* 2001;86:4163-4166.
17. Nisisako T, Torii T, Higuchi T. Droplet formation in a microchannel network. *Lab Chip.* 2002;2:24-26.
18. Dreyfus R, Tabeling P, Willaime H. Ordered and disordered patterns in two-phase flows in microchannels. *Phys Rev Lett.* 2003;90:144505/1-4.
19. Tice JD, Lyon AD, Ismagilov RF. Effects of viscosity on droplet formation and mixing in microfluidic channels. *Anal Chim Acta.* 2004;507:73-77.
20. Cristini V, Tan YC. Theory and numerical simulation of droplet dynamics in complex flows—A review. *Lab Chip.* 2004;4:257-264.
21. Joscelyne SM, Tragardh G. Membrane emulsification—A literature review. *J Membr Sci.* 2000;169:107-117.

Manuscript received Feb. 13, 2006, and revision received Apr. 28, 2006.